Astron. Astrophys. 356, 1149–1156 (2000)

ASTRONOMY AND ASTROPHYSICS

Free-free and recombination radiation from massive star-forming regions

T. Beckert[1,2], **W.J. Duschl**[1,3], **and P.G. Mezger**[3]

[1] Institut für Theoretische Astrophysik, Tiergartenstrasse 15, 69121 Heidelberg, Germany
[2] Center for Astrophysics, 60 Garden Street, Cambridge, MA 02138, USA
[3] Max-Planck-Institut für Radioastronomie, Auf dem Hügel 69, 53121 Bonn, Germany

Received 26 August 1999 / Accepted 25 February 2000

Abstract. The contribution of free-free and recombination radiation to the IR emission from regions of massive star formation is investigated. A method for calculating Gaunt factors for free-free emission from a hydrogenic non-relativistic gas is employed and the results are compared with approximation formula from the literature. While the cooling of ionized star forming regions due to free-free and free-bound transitions emerges in the MIR, which is dominated by dust emission, the overall cooling is mainly provided by line emission of heavier elements. Only in metal-free and therefore dust-free H II regions can free-free and free-bound radiation become dominant. We investigate the global energy balance of those regions and determine temperatures of the ionized gas, which are in general 2 to 8 times larger than found in present day star forming regions of massive stars.

Key words: radiation mechanisms: thermal – ISM: H II regions – infrared: ISM: continuum – radio continuum: general – radio continuum: ISM

1. Introduction – The radio/IR emission from star-forming regions

Massive stars are preferentially formed in dense cores of molecular clouds. Photons emitted by the stars beyond the Lyman continuum (Lyc) limit ($\lambda \leq 912$ Å) ionize the surrounding gas, which emits the absorbed energy as free-free, free-bound and – after recombination – as bound-bound emission. The recombined and still excited atoms decay to the ground state faster than they are reionized.

In this paper we present a calculation from first principles of the free-free emission for the case of a non-relativistic hydrogen gas, including recombination radiation. We compare the results with widely used analytical approximations for the low and the high frequency limits. Our results yield a consistent description of the Gaunt factor for the entire frequency range. In particular, the domain between the low and the high frequency approximations around 10^3 GHz is of interest for a comparison between free-free and dust emission from H II regions.

In describing H II regions it is usually assumed (but is correct only for electron densities $n_{\rm e} \gg 2\,10^3\,{\rm cm}^{-3}$) that all Lyc-photons absorbed by the gas, $N'_{\rm Lyc}$, decay into Ly$_\alpha$ photons ($N_\alpha \sim N'_{\rm Lyc}$) which eventually get absorbed by dust inside and surrounding the H II region. Stellar radiation $S_{*,\nu<\nu_{\rm Lyc}}$ longward of the Lyc-limit

$$S_{*,\nu<\nu_{\rm Lyc}} = \sum_i n_i B_\nu(T_{{\rm eff},i})\pi R_i^2 \quad \text{with} \quad \nu < \nu_{\rm Lyc} \tag{1}$$

is absorbed by dust in the compact H II region (absorption optical depth τ_1) and in the molecular cloud (τ_2) or alternatively escapes to reach the observer. n_i is the column density of stars of a given spectral type i and R_i their radius. Free-free and free-bound emission

$$S_{\rm ff+} = B_\nu(T_{\rm e})(1 - {\rm e}^{-\tau_{\nu,{\rm ff+}}}) \tag{2}$$

is absorbed by dust in the molecular cloud, where here and in the following ff+ implies the sum of free-free and free-bound transitions. We neglect absorption of ff+ emission by dust inside the H II region. Dust gets heated by absorption of direct and indirect stellar radiation to an average dust temperature $T_{\rm d}$ resulting in thermal emission from dust

$$S_{\rm d} = B_\nu(T_{\rm d})(1 - e^{-\tau_{\nu,{\rm d}}}). \tag{3}$$

Hence the total continuum emission of an HII region is

$$S_\nu({\rm H\,II}) = \left(S_{*,\nu<\nu_{\rm Lyc}} e^{-\tau_1} + S_{\rm ff+}\right) e^{-\tau_2} + S_{\rm d}. \tag{4}$$

with $B_\nu(T_{\rm e}) = 2h\nu^3 c^{-2}/\left(\exp\left[h\nu/kT_{\rm e}\right] - 1\right)$ the Planck function and $T_{\rm e}$ the electron temperature in the ionized gas. The use of the Planck function for free-free emission is valid only for thermal electron distributions and must be replaced by a general source function otherwise. This is treated in Sect. 2. Typical parameters of H II regions are $T_{\rm e} \sim 6 - 8\,10^3$ K and $T_{\rm d} \leq 400$ K. Stellar temperatures of ionizing stars (spectral type B0 and earlier) are $T_{\rm eff} \geq 3\,10^4$ K producing an emission

Send offprint requests to: W.J. Duschl, Institut für Theoretische Astrophysik, Tiergartenstrasse 15, 69121 Heidelberg, Germany (wjd@ita.uni-heidelberg.de)
Correspondence to: W.J. Duschl, Institut für Theoretische Astrophysik, Tiergartenstrasse 15, 69121 Heidelberg, Germany (wjd@ita.uni-heidelberg.de)

rate of ionizing photons $N_{\rm Lyc} \geq 4\,10^{47}{\rm s}^{-1}$ and luminosities $L_* \geq 3\,10^4\,{\rm L}_\odot$. Usually free-free emission dominates the radio spectrum ($\nu \leq 10^{11}$ Hz), dust emission the submm through MIR regime ($10^{11} \leq \nu/{\rm Hz} \leq 5\,10^{13}$) and stellar and/or free-bound emission the NIR continuum ($5\,10^{13} \leq \nu/{\rm Hz} \leq 3\,10^{14}$). Dust ($T_{\rm d} \leq 400\,{\rm K}$) affects the NIR spectrum mainly by absorption as shown in Eq. 4.

About thirty years ago it was realized that Eq. 4 – applied to the observed spectrum of planetary nebulae and compact H II regions – can be used to determine the stellar parameters L_* and $N_{\rm Lyc}$ as well as the extinction of dust located in front of the ionizing stars. From the free-free flux density at a radio frequency where $\tau_{\rm ff+} \leq 1$, one can predict $S_{\rm ff+}$ at NIR wavelengths and estimate with Eq. 4 dust absorption or stellar radiation. Willner et al. (1972) – using the Gaunt factor computed and tabulated by Karzas & Latter (1962) – applied this observing strategy to planetary nebulae and found in most cases excess emission at NIR wavelengths, which they attributed to very hot ($T_{\rm d} \sim 1000\,{\rm K}$) dust. Wynn-Williams et al. (1972) observed and compared the radio and MIR/NIR emission from compact H II regions located in the giant H II region W 3. They modeled the $\lambda\,3 - 20\,\mu$m part of the spectrum with emission from 150 K dust mixed with the ionized gas, and explained a deficiency of the observed K-band ($\lambda\,2.2\,\mu$m) flux density by dust absorption of up to $A_{\rm V} \sim 50^{\rm m}$. Both investigations indicated that free-free and free-bound emission dominate the emission in the NIR regime. Only in one case was excess NIR emission observed and attributed to a point source, thought to be a heavily obscured O star.

In the following we consider the contribution of free-free and free-bound radiation from radio to NIR wavelengths emission. We compute the spectra of ionized gas in Sects. 2 and 3, and discuss its contribution to the spectrum and total luminosity of an H II region in Sect. 4. We find the most interesting application in metal-free H II regions which we treat in Sect. 5. We present our conclusions in Sect. 6.

2. Free-free emission

Free-free emission, or Bremsstrahlung, is emitted as electrons are scattered by ions. The emissivity can be derived in a semiclassical way due to Kramers and Wentzel (Kramers 1923), which deviates from the exact quantum mechanical treatment. Gaunt (1930) quantified the ratio of the exact to the semiclassical value by introducing a corresponding factor which today usually is named after him the *Gaunt factor*. For radio observations of H II regions the low-frequency limit (LFL; $\nu \lesssim 10\,{\rm GHz}$) of the Gaunt factor is sufficient, while at IR-wavelength the emissivity deviates considerably from the LFL and from the high energy approximation of Menzel & Pekeris (1935). The ff+ spectrum is given by Eq. 2. For $T_{\rm e} \sim 6 - 8\,10^3\,{\rm K}$ and $\nu \leq 10^{13}\,{\rm Hz}$ the Raleigh-Jeans approximation $B_\nu(T) \propto \nu^2$, and for $\nu \geq 10^{15}\,{\rm Hz}$ the Wien approximation $B_\nu(T) \propto \nu^3 \exp(-h\nu/kT)$ apply. The optical depth in the R-J limit decreases with ν and $T_{\rm e}$ according to

$$\tau_{\nu,{\rm ff+}} = 3.014\,10^{16} \left(\frac{\nu}{\rm Hz}\right)^{-2} \left(\frac{T_{\rm e}}{\rm K}\right)^{-1.5} \left(\frac{EM}{\rm pc\,cm^{-6}}\right) g_{\rm ff+} \quad (5)$$

with $EM = \int n_{\rm e}^2 {\rm d}l$ the emission measure. $g_{\rm ff+}$ is the Gaunt factor for free-free and free-bound transitions averaged over a Maxwellian velocity distribution which in its rigorous form is rather difficult to handle. There exist a number of approximations for different regimes in $(T_{\rm e}, \nu)$-space, see for instance the work of Brussaard & van de Hulst (1962) and Karzas & Latter (1962).

2.1. Rigorous treatment of free-free emission

For $T_{\rm e} \sim 10^4\,{\rm K}$ the free-free contribution to the emission in H II regions requires a detailed treatment. The cross section for the emission of one photon is

$$ {\rm d}\sigma_{\rm ff} = \frac{16\pi}{3\sqrt{3}} \alpha^3 Z_1^2 Z_2^2 \left(\frac{\hbar}{mv}\right)^2 g(\eta_{\rm i}, \eta_{\rm f}) \frac{{\rm d}\nu}{\nu} \quad (6)$$

with the Gaunt factor g as the ratio of the quantum mechanical cross section to the semiclassical result of Kramers and Wentzel. In this context α is the fine structure constant, Z_1 the charge of the ion which is assumed to be hydrogenic, Z_2 the charge, m the mass and v the velocity of the electron. Grant (1958) derived the Gaunt factor using Coulomb wave functions for initial and final states of free electrons in the form

$$g(\eta_{\rm i}, \eta_{\rm f}) = \frac{\eta_{\rm i}\eta_{\rm f}}{|\eta_{\rm i} - \eta_{\rm f}|} \frac{\sqrt{3}\pi\,|\Delta(i\eta_{\rm i}, i\eta_{\rm f})|}{(\exp[2\pi\eta_{\rm f}] - 1)(1 - \exp[-2\pi\eta_{\rm i}])} \quad (7)$$

with the complex function

$$\Delta(i\eta_{\rm i}, i\eta_{\rm f}) = \quad (8)$$
$$(F(1 - i\eta_{\rm i}, -i\eta_{\rm f}, 1, z))^2 - (F(1 - i\eta_{\rm f}, -i\eta_{\rm i}, 1, z))^2$$

expressed by hypergeometric functions F. This result was stated earlier by Menzel & Pekeris (1935) in a different way. The parameters $\eta_{\rm i}$ and $\eta_{\rm f}$ are related to the electron velocities by

$$\eta_{\rm f,i} = \alpha Z_1 Z_2 \frac{c}{v_{\rm f,i}}, \qquad z = -4\frac{\eta_{\rm i}\eta_{\rm f}}{\xi^2}, \quad \text{and} \quad \xi = \eta_{\rm f} - \eta_{\rm i}. \quad (9)$$

The indices refer to the initial (i) and final (f) state of the electron. The derivation of Eq. 7 assumes a point-like scattering object. Accordingly it is strictly correct only for fully ionized atoms, like H^+, He^{++}, ... This Gaunt factor of Eq. 7 is used in the numerical treatment below.

2.2. Thermally averaged Gaunt factors

In many cases the electrons can be assumed to obey a thermal distribution of temperature $T = T_e$ and the free-free emission stated in Eq. 13 of a dilute thermal plasma is obtained from the Maxwellian average of the Gaunt factor (see Appendix A) by

$$g_{\rm ff} = \int_0^\infty g(\eta_{\rm i}, \eta_{\rm f}) e^{-y}\,{\rm d}y \quad (10)$$

with the dimensionless kinetic energy of the electrons after scattering scaled to the mean electron energy $\langle\mathcal{E}\rangle$

$$y = \left(mv_{\rm i}^2/2 - h\nu\right) / \langle\mathcal{E}\rangle\,. \quad (11)$$

The spectral emissivity depends on frequency through the Gaunt factor times the exponential $\exp[-h\nu/kT]$ which follows since only electrons with initial energies in excess of $h\nu$ contribute to the emissivity (see also Appendix A). The free-free emissivity is given by

$$\epsilon_\nu = n_e n_i \int_{v_0}^{\infty} \left(\frac{\mathrm{d}\sigma_{\mathrm{ff}}}{\mathrm{d}\nu}\right) \frac{h\nu}{4\pi}\, v_{\mathrm{i}}\, f(v_{\mathrm{i}})\, \mathrm{d}v_{\mathrm{i}}. \quad (12)$$

Inserting Eqs. 6 and 10 results in

$$\epsilon_\nu = n_e n_i \frac{8}{3}\left(\frac{2\pi}{3}\right)^{1/2} \frac{e^6 Z_i^2}{(mc^2)^{3/2}}\,(kT)^{-1/2}\, e^{-\frac{h\nu}{kT}}\, g_{\mathrm{ff}}. \quad (13)$$

The corresponding optical depth for thermal electrons is

$$\tau_{\mathrm{ff}} = \frac{4}{3}\left(\frac{2\pi}{3}\right)^{1/2} r_e^3 \frac{Z_i^2 m^{3/2} c^5}{(kT)^{1/2}\; h\nu^3}\left(1 - e^{-\frac{h\nu}{kT}}\right) g_{\mathrm{ff}}\; EM \quad (14)$$

$$\begin{aligned}\tau_{\mathrm{ff}} \;&=\; 1.13725\left(1 - e^{-\frac{h\nu}{kT}}\right) g_{\mathrm{ff}} \\ &\times\; \left[\frac{T}{\mathrm{K}}\right]^{-\frac{1}{2}} \left[\frac{\nu}{\mathrm{GHz}}\right]^{-3} \left[\frac{EM}{\mathrm{pc\,cm^{-6}}}\right]. \end{aligned} \quad (15)$$

In the Rayleigh-Jeans limit we obtain optical depth

$$\tau_{\mathrm{ff}} = \frac{4}{3}\left(\frac{2\pi}{3}\right)^{1/2} r_e^3 Z_i^2 \left(\frac{mc^2}{kT}\right)^{3/2} \frac{c^2}{\nu^2}\, g_{\mathrm{ff}}\; EM \quad (16)$$

which is the free-free contribution ($g_{\mathrm{ff}+} = g_{\mathrm{ff}} + g_{\mathrm{fb}}$) in Eq. 5.

2.3. Numerical methods

The hypergeometric functions entering in Eq. 8 assume a large negative argument z with $|z| \gg 1$ for most frequencies of interest $h\nu \ll \mathcal{E}_{\mathrm{f}} < \mathcal{E}_{\mathrm{i}}$ with $\mathcal{E}_{\mathrm{i}}$ and $\mathcal{E}_{\mathrm{f}}$ the initial and final energy, respectively. To obtain an argument inside the unit circle in the complex plane we make use of a linear transformation of the hypergeometric function (e.g., Abramowitz & Stegun 1972)

$$\begin{aligned} &F(a,b,1,z) \\ &= \frac{\Gamma(-(1\pm i\xi))}{\Gamma(b)\Gamma(1-a)}(-z)^{-a} F(a,a,2\pm i\xi,1/z) \quad (17)\\ &\quad - \frac{\Gamma(1\pm i\xi)}{\Gamma(a)\Gamma(1-b)}(-z)^{-b} F(b,b,\mp i\xi,1/z) \\ &\quad a = 1 - i\eta_{\mathrm{i,f}} \qquad b = -i\eta_{\mathrm{f,i}} \quad (18)\end{aligned}$$

which is especially useful for a numerical treatment. The complex Δ-function defined in Eq. 8 is evaluated with the hypergeometric series for $F(a,b,c,z)$ which has a good numerical convergence if

$$|z| < z_{\mathrm{c}} = \min\left(0.1\left|c(ab)^{-1}\right|, 0.1\right). \quad (19)$$

This is sufficient for very high frequencies but does not dominate the thermal average. If $|z| > z_c$ we can take $\exp[i\arg(z)]z_{\mathrm{c}}$ as the starting argument for the hypergeometric series and continue to solve the hypergeometric differential equation by the Bulirsch-Stör method. If the value of $-z$ exceeds 0.5 we choose the transformation given in Eq. 17, because we find that the step-size of the integration scheme does not underflow in that case. For very large $|z|$ the approximation of Eq. 23 can be employed preventing numerical inaccurate results. This scheme provides the argument for the integration in Eq. 10. The integration uses the extended midpoint rule and a split of the y-axis at a midpoint $y_0 = 1$

$$\begin{aligned} g_{\mathrm{ff}} \;&=\; \int_0^{y_0} g(\eta_{\mathrm{i}}(y), \eta_{\mathrm{f}}(y))\exp(-y)\;\mathrm{d}y \quad (20)\\ &\quad + \int_0^{1/y_0} g(\eta_{\mathrm{i}}(1/y), \eta_{\mathrm{f}}(1/y))\frac{\exp(y)}{y^2}\;\mathrm{d}y. \end{aligned}$$

All Gaunt factors shown in the attached figures are calculated in this way if not stated otherwise. In Fig. 1 we compare our results for a temperature of $7\,10^3$ K with approximations for the LFL and the high energy limit. For different temperatures we always find a frequency interval where both approximations are in error by more than 10 %. The method presented here can be used for an accurate calculation of free-free Gaunt factors for a wide range of temperatures and frequencies as shown in Fig. 3. In Table 1 we summarize the validity ranges of often used analytical approximations.

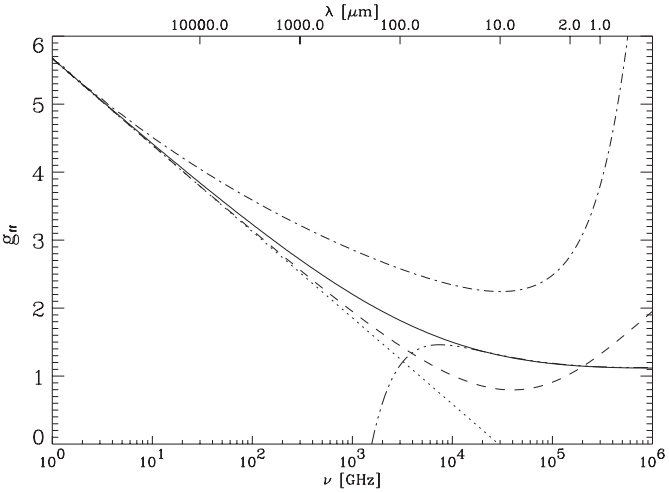

Fig. 1. The Gaunt factor g_{ff} for free-free radiation according to Eqs. 10 and 7 calculated in the way described in Sect. 2.3. This is shown as the solid line and is the most accurate calculation. We choose $T_{\mathrm{e}} = 7\,10^3$ K, i.e., a typical value for H II regions. The dotted line represents the classical approximation of Scheuer (1960) and Oster (1961), while the dashed curve is due to Eq. 23. The high-energy limit of Menzel & Pekeris (1935) is shown as dashed-3×dotted and the low frequency limit fit of Altenhoff et al. (1960) is dash-dotted.

2.4. Low-frequency limit

Of special interest for radio observations is the low-frequency limit, where the frequency of the emitted photon is much smaller than the final energy $\mathcal{E}_{\mathrm{f}}$. So we can introduce a variable

$$x = \frac{h\nu}{\mathcal{E}_{\mathrm{f}}} \quad (21)$$

Table 1. Validity ranges for often used analytic approximations to the Gaunt factor for temperatures in the range of $\approx 10^{2.3}$ to $\approx 10^{4.2}$ K.

Frequency range	Approximation by
$\lesssim 10$ GHz	Altenhoff et al. (1960)
$\lesssim 10^2$ GHz	Scheuer (1960), Oster (1961)
$\gtrsim 10^4$ GHz	Menzel & Pekeris (1935)

and explore the Gaunt factor in the limit $x \to 0$. This corresponds to

$$z = -4\frac{\sqrt{1+x}}{\left(\sqrt{1+x}-1\right)^2} \to -\infty \tag{22}$$

and allows the use of the hypergeometric series for the evaluation of Eq. 17. For large $-z$ the series converges rapidly and can be used for numerical purposes, if η_f is not too large. Expanding $\Delta(\eta_\mathrm{i}, \eta_\mathrm{f})$ to first order in x we get the absolute value of $g(\eta_\mathrm{i}, \eta_\mathrm{f})$ in this limit

$$g(\eta_\mathrm{i}, \eta_\mathrm{f}) = \frac{\sqrt{3}}{\pi}\left|\gamma - \log(4/x) + \Re\left(\Psi(i\eta_\mathrm{f})\right)\right| \tag{23}$$

which was obtained by Oster (1963) as an exact result. We rather derive this result as the limiting case for $h\nu \ll \mathcal{E}_\mathrm{f}$. In the LFL, which corresponds to $\eta_\mathrm{f} \to 0$ the real part of the Digamma-Function, $\Psi(i\eta_\mathrm{f})$, is approximately $-\gamma = 0.5772\ldots$ and we obtain the classical value

$$g(\eta_\mathrm{i}, \eta_\mathrm{f}) = \frac{\sqrt{3}}{\pi}\log(4/x). \tag{24}$$

For H II regions and $\nu \leq 10^{11}$ Hz the LFL of Eq. 24 can be used in the thermal average. The corresponding approximation

$$g_\mathrm{ff} = \ln\left[4.955\,10^6(\nu/\mathrm{Hz})^{-1}\right] + 1.5\ln(T_\mathrm{e}) \tag{25}$$

derived by Oster (1961, 1970) is widely used. For the radio regime there exists an even simpler approximation by Altenhoff et al. (1960) which, combined with Eq. 5, yields

$$\begin{aligned}\tau_\mathrm{c} &= 7.94\,10^{16}\left(\frac{T_\mathrm{e}}{\mathrm{K}}\right)^{-1.35}\left(\frac{\nu}{\mathrm{Hz}}\right)^{-2.1} \\ &\times \left(\frac{E}{\mathrm{pc\,cm^{-6}}}\right) a(\nu, T_\mathrm{e})\end{aligned} \tag{26}$$

with a correction factor $a(\nu, T_\mathrm{e})$ (Mezger & Henderson 1967) which accounts for the difference between this approximation and the one by Oster (1961).

We have computed and show in Fig. 1 the averaged Gaunt factor together with its approximations by Oster and Altenhoff et al., respectively.

3. Free-bound transitions

Free-bound transitions provide a considerable fraction to the NIR-emission of H II regions. Our aim is to recapitulate the existing theory and combine it with the free-free emission. We assume thermodynamic equilibrium, allowing Saha's equation to be used. From this, one obtains the Milne relation

$$\frac{\sigma_\mathrm{fb}}{\sigma_\mathrm{bf}} = \frac{2(h\nu)^2}{(mc^2)(mv^2)}\frac{g_\mathrm{n}}{g_\mathrm{e}g_+}. \tag{27}$$

Karzas & Latter (1962) obtained for hydrogenic atoms the cross section

$$\sigma_\mathrm{bf} = \frac{512\pi^7 m e^{10} Z^4}{3\sqrt{3}c\omega^3 h^6 n^5} g(\omega, n, l, Z) \tag{28}$$

with a Gaunt factor $g(\omega, n, l, Z)$ depending on the radial and angular quantum numbers (n, l). This Gaunt factor is usually of order unity. The number of emitted photons

$$N_+ N_\mathrm{e}\sigma_\mathrm{fb}\, f(v)\, v\, \mathrm{d}v \tag{29}$$

times $h\nu\delta(\nu - \xi/h - mv^2/2)\mathrm{d}\nu$ integrated over the electron velocity distribution results in

$$\epsilon_{(n,\nu)}\mathrm{d}\nu = N_\mathrm{e}N_\mathrm{i}\frac{A}{(kT)^{3/2}}\frac{\bar{g}}{n^3}\exp\left[-\frac{h\nu}{kT} + \frac{\chi}{n^2 kT}\right]\mathrm{d}\nu \tag{30}$$

$$A = \frac{16\sqrt{2\pi}Z^2 e^6\sqrt{m}}{3\sqrt{3}m^2c^3}\chi \qquad \chi = \frac{2\pi^2 m e^4 Z^2}{h^2} \tag{31}$$

which is the emissivity for radiative recombinations to states of radial quantum number n. The spectral emissivity for all recombinations is the sum over all transitions to ionization energies χ/n^2 less than the photon energy. So

$$\epsilon_\nu = \sum_{n\geq k}^{\infty}\epsilon_{(n,\nu)} \qquad k = \sqrt{\chi/h\nu} \tag{32}$$

is the free-bound emissivity for hydrogenic ions of charge Z. For the sake of convenience we use the approximation of Brussaard & van de Hulst (1962) to evaluate the sum in Eq. 32. The emission spectrum of free-free and free-bound transitions has been combined in Fig. 2. At NIR-frequencies the free-bound radiation dominates over free-free emission.

4. Recombination line emission and energetic considerations

In H II regions all electrons captured via free-bound transitions produce a cascade of recombination lines which can be observed from radio to optical frequencies. Lines in recombination cascades contribute to the cooling of the H II region. Accurate emissivities with Gaunt factors for recombination lines depending on temperature and densities in the range of interest are tabulated in machine-readable form (Storey & Hummer 1995). The Lyc photons produced by stars heating the H II region are captured in the gas where ionization from and recombination to the ground state of H I balance each other (Rubin 1968) so that for a static ionized region

$$N_\mathrm{Lyc} = \int \mathrm{d}V\; n_\mathrm{e}n_\mathrm{i}(\beta_\mathrm{tot} - \beta_1). \tag{33}$$

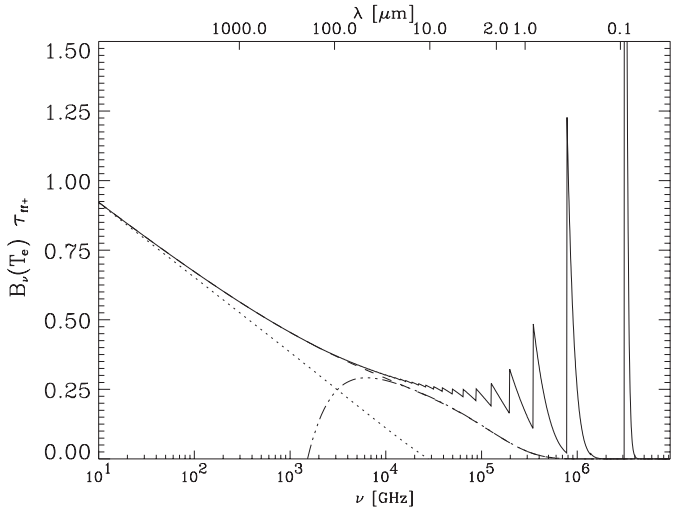

Fig. 2. The spectrum of free-free and free-bound radiation (solid line), which has been scaled to unity for $\nu = 5$ GHz. We take $T_\mathrm{e} = 7\,10^3$ K. The dotted line represents the classical approximation by Oster (1961). The free-free emission alone is shown as dashed line. The low-energy limit of Menzel & Pekeris (1935) is shown as dashed-3×dotted.

The cooling proceeds via recombination to quantum levels $n > 1$ and subsequent line emission. The quantity β_n is the rate coefficient of recombination on level n and β_tot the total recombination coefficient. The value $\beta_\mathrm{tot} - \beta_1$ can be obtained from Seaton (1959) to an accuracy of a few per cent for $T < 2\,10^4$ K as

$$\beta_\mathrm{tot} - \beta_1 = 4.10\,10^{-10} T^{-0.8} \mathrm{cm^3 s^{-1}}. \quad (34)$$

The mean energy of Lyc photons of OB-star clusters varies from $1.72 h\nu_\alpha$ for B0-stars to $2.41 h\nu_\alpha$ for O4-stars resulting in a mean value of $2.30 h\nu_\alpha$ (Mezger et al. 1974) with $h\nu_\alpha$ the energy of Ly$_\alpha$ photons.

In the following, we will concentrate on ionization-bounded H II regions which – on average – are heated by

$$\begin{aligned} L_{*,\lambda<91.2\mathrm{nm}} &= 3.76\,10^{-11} N_\mathrm{Lyc} \\ &= 1.29\,10^{-23} V n_e^2 \left[\frac{T_e}{7\,10^3\,\mathrm{K}}\right]^{-0.8} \mathrm{erg\,s^{-1}} \end{aligned} \quad (35)$$

if the volume is measured in cm^3 and the electron density in cm^{-3}. For typical temperatures of $T_\mathrm{e} \sim 7\,10^3$ K, the Lyc luminosity of the stars is larger than the luminosity of free-bound emission from recombination onto ground state, which is obtained by integrating Eq. 30 for $n = 1$ over frequencies. This results in (Cooper 1966)

$$L_{\mathrm{fb},n=1} = 4.50\,10^{-22} V n_e^2\, T^{-0.5}\, \langle g_\mathrm{fb}\rangle \,\mathrm{erg\,s^{-1}} \quad (36)$$

with the integrated Gaunt factor for free-bound emission

$$\langle g_\mathrm{fb}\rangle = e^\xi \int_\xi^\infty \mathrm{d}u\; g_\mathrm{fb}\; e^{-u} \qquad \xi = \frac{\chi}{n^2 kT}. \quad (37)$$

Numerically we find $\langle g_\mathrm{fb}\rangle = 0.855$ for $T_\mathrm{e} = 7\,10^3$ K. The cooling of the H II region proceeds partly by electrons recombining on quantum levels $n > 1$. The corresponding luminosity is easily seen to be

$$L_{\mathrm{fb},n>1} = (\zeta(3) - 1)\, \frac{\langle g_\mathrm{fb}\rangle_{n>1}}{\langle \bar{g}\rangle} L_{\mathrm{fb},n=1} \quad (38)$$

and amounts to 25% of $L_{\mathrm{fb},n=1}$ again for $T_\mathrm{e} = 7\,10^3$ K. ζ is known as the Riemann-ζ-function. The contribution of free-free emission to the cooling rate of the H II region can be neglected at the temperatures under consideration. At $7\,10^3$ K the free-free contribution is just 2% of the free-bound radiation. The last radiative contribution to the cooling radiation from hydrogen is provided by bound-bound transitions after recombination. As ionization-bounded regions are optically thick for Lyc photons every ionizing photon from the star ends up as a photon in the Lyman series while exited atoms decay to ground state. Here one has to distinguish between regions optically thin (case A) or thick (case B) in the Lyman lines.

In case A the most energetic photons in lines are Ly$_\alpha$ photons. We approximate the bound-bound luminosity by multiplying the Ly$_\alpha$ energy with the number of Lyc photons originally available, and obtain

$$L_\mathrm{bb} = 1.63\,10^{-11} N_\mathrm{Lyc}\,\mathrm{erg\,s^{-1}}. \quad (39)$$

For proton densities $N_\mathrm{p} \le 10^4$ cm^{-3} the $2\,^2S$ level of hydrogen is depopulated by two-photon decay. This produces continuum radiation which is probably optically thin, so that the energy radiated by bound-bound transitions in Case A and B is still reasonably well approximated by Eq. 39. If we take an evolved H II region, assuming it is ionization-bounded and therefore that its size is that of the Strömgren sphere, the sum of all cooling processes under discussion accounts for 70% to 75% of the cooling between 6000 and 14000 K

$$L = L_{\mathrm{fb},n>1} + L_\mathrm{bb} + L_\mathrm{ff} = 0.72 L_{*,\lambda<91.2\,\mathrm{nm}} \quad (40)$$

and can provide the total cooling of the H II region. If free-bound, free-free, and bound-bound emission from an ionized hydrogen gas would have to balance the heating of the star given in Eq. 35, the gas temperature would be as high as $T \sim 5.7\,10^4$ K. A similar temperature is derived from balancing electron heating due to ionization inside the largely ionized gas derived below in Eq. 47 and free-free emission, which cools free electrons without destroying them. This gives a temperature of $4\,10^4$ K for the electrons independent of density and size of the ionized region. However, additional cooling is provided by forbidden line emission from collisionally excited atoms of heavier elements. These metals determine the temperature of the gas in stationary H II regions.

5. Metal-free H II regions

An ionization-bounded H II region with primordial abundancies of hydrogen and helium, but without heavier elements, must be much hotter than present day H II regions as shown in the previous section. Even then, not all ionizing photons will be absorbed and converted to soft photons, but reach the actual

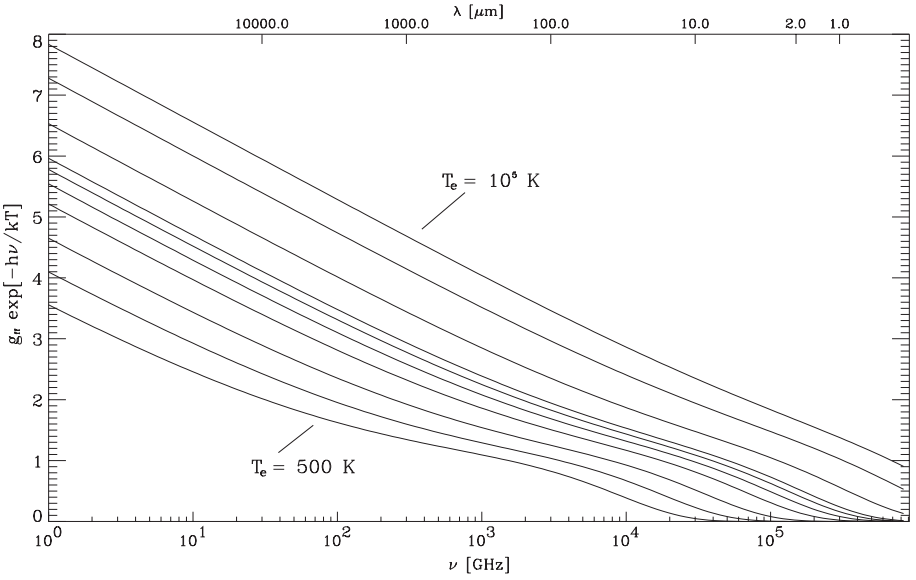

Fig. 3. Frequency dependence of the free-free emissivity $\epsilon_\nu \propto g_{\rm ff} \exp[-h\nu/(kT)]$ for different $T_{\rm e}/{\rm K} = \{5\,10^2,\ 10^3,\ 2\,10^3,\ 4\,10^3,\ 6\,10^3,\ 8\,10^3,\ 10^4,\ 5\,10^4,\ 10^5\}$.

boundary of the H II region and drive an ionization front into the surrounding neutral gas. Some fraction $1-e^{-\tau}$ of the stellar Lyc luminosity L_* is consumed at the front for ionization and heating of the gas. We approximate the ionizing spectrum of the star and the radiation at the front by a Wien-law of temperature $T_{\rm eff}$. The gas heating at the front is then

$$L_{\rm hf} = 8\pi R_s^2 \frac{k^2 T_{\rm eff}^2 \nu_0^2}{hc^2} \exp\left[-\frac{h\nu_0}{kT_{\rm eff}}\right] e^{-\tau} \tag{41}$$

which also suffers from losses inside the ionized region by an opacity factor $\exp(-\tau)$. If we set up the energy balance for the ionizing photons injected by the star, we find a minimal temperature such that τ is real, but can balance the energy budget for any temperature above that. The number of ionizing photons is reduced in the H II region only by free-bound transitions, which equal the number of recombinations determined by Eq. 34 in ionization equilibrium. The total energy balance is then

$$L_*(1-e^{-\tau}) + L_{\rm hf} = L_{\rm ff} + L_{\rm fb} + L_{\rm bb} \tag{42}$$

$$\exp[-\tau] = \frac{V n_e n_i (\beta_{\rm tot} - \beta_1)}{N_{\rm Lyc}} \tag{43}$$

with the recombination rate given by Eq. 34 and the cooling from Eqs. 39 and 38. The free-free luminosity

$$L_{\rm ff} = 1.42\ 10^{-27} n_{\rm e} n_{\rm i} V \langle g_{\rm ff}\rangle \sqrt{T_{\rm e}} \tag{44}$$

includes the spectral averaged Gaunt factor $\langle g_{\rm ff}\rangle$. The balance Eq. 42 has two solutions: One at high temperatures of several 10^6 K, where the cooling is dominated by free-free emission, and another one between 10^4 and a few 10^5 K, where the cooling is due to free-bound and bound-bound transitions. In both cases the equilibrium temperature is very sensitive to density and radius or the product $n_e^2 R^3$ of the H II region. The high temperature solution faces two severe problems in our context. The expansion time for the ionization front driven by a massive star is of the order of 10^6 years while the recombination time scale for reaching ionization balance in a region of mean density $n_e = 10^2\,{\rm cm}^{-3}$ and temperatures of a few 10^6 K is itself 10^6 years. So we cannot expect an ionization equilibrium to hold in this case and the determination of an equilibrium temperature is time dependent. The second conjecture comes from the thermal balance of the electrons alone. The main cooling of free electrons in our situation is provided by free-free emission while the heating takes place at the ionization front (Eq. 41) and by reionization inside the H II region after recombination. The energy gain in the ionized region is proportional to the recombination rate in equilibrium and the mean energy of a new electron created by ionization. We neglect the energy of recombining electrons here. The mean energy of a new electron is determined by the ionizing spectrum, taken to follow a Wien law and the absorption cross section, which declines steeply as ν^{-3} close to the ionization edge. From that we get the mean energy as

$$\mathcal{E} = \frac{kT_{\rm eff}\exp[-x] - h\nu_0 E_1(x)}{E_1(x)} \approx kT_{\rm eff}\frac{x-2}{x-1} \tag{45}$$

with

$$x = \frac{\chi}{kT_{\rm eff}}, \tag{46}$$

the energy of the ionization edge χ from Eq. 31 and the exponential integral $E_1(x)$ (e.g., Abramowitz & Stegun 1972). The approximation in Eq. 45 holds only for low effective stellar temperatures $kT_{\rm eff} \ll \chi$. The inside heating of H II regions is

$$L_{\rm h} = n_{\rm e} n_{\rm i} V \mathcal{E} (\beta_{\rm tot} - \beta_1) \tag{47}$$

and we get an approximate electron energy balance

$$L_{\rm ff} = L_{\rm h} + L_{\rm hf}, \tag{48}$$

which is only satisfied to within a factor of two for $\exp(-\tau)$ present in Eq. 41 in case of the lower temperature solution. The electron energy balance Eq. 48 cannot hold for the high energy

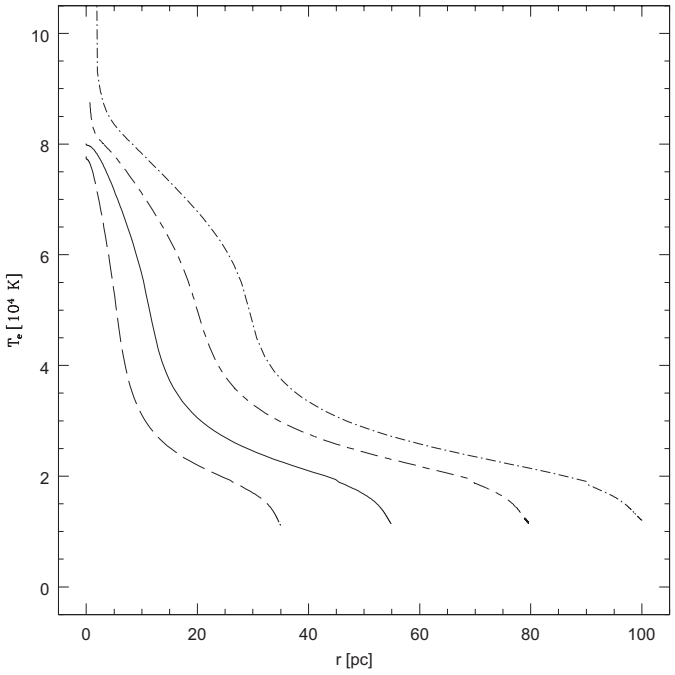

Fig. 4. T_e of H II regions of primordial composition. The central ionizing source is a black body of $3.0\,10^4$ K (dashed), $3.5\,10^4$ K (solid), $3.8\,10^4$ (long-short dashed) and $4.5\,10^4$ K (dash-dotted curve). r is the radial distance from the ionizing star. The density structure of the H II and the parameters of the central star are given in the text.

solution. In that case the free-free cooling rises with temperature while the recombination rate declines and the gas heating at the ionization front is more or less independent of T_e in the H II region. The opacity τ due to conversion of photons inside the ionized region becomes less important with increasing temperature.

For illustration we have performed a simplified 1D radiative transfer and ionization balance calculation including hydrogen and helium. The local calculation finds only the lower temperature solution. We have taken a density distribution with a central cusp

$$n_\mathrm{H} = n_0 \left(1 + (r/r_0)^2\right)^{-1} + n_1 \tag{49}$$

with $n_0 = 10^6\,\mathrm{cm}^{-3}$ and $n_1 = 1\,\mathrm{cm}^{-3}$ and a cusp radius of $r_0 = 10^3 R_*$ for central stars with effective temperatures of $3\,10^4$ K with $R_* = 10\,\mathrm{R}_\odot$, $3.5\,10^4$ K with $R_* = 12\,\mathrm{R}_\odot$, $3.8\,10^4$ K with $R_* = 16\,\mathrm{R}_\odot$ and $4.5\,10^4$ K with $R_* = 14\mathrm{R}_\odot$. The stellar spectrum is approximated by a black body. The density reaches a constant value beyond $r = 10^6 R_* \approx 0.4$ pc. The derived temperature profiles are shown in Fig. 4.

6. Conclusions

We have demonstrated the importance of detailed calculations for thermal Gaunt factors of free-free emission. While the usual approximations in the radio and IR spectral bands are sufficient, there is a gap in frequencies where one has to rely on tabulated values or use a more sophisticated method as suggested here. For wavelength less than 100 μm free-bound transitions start to dominate over bremsstrahlung for $T_\mathrm{e} < 10^4$ K. We have not gone beyond the standard formula for the free-bound transition but provide a short summary of that process. Despite their importance from the radio to NIR energy bands the total cooling of present day H II regions around massive stars is supported by line emission of heavier elements as is well known (Osterbrock 1989). We show that free-free, free-bound and subsequent bound-bound radiation can account for roughly 70% of the cooling. The first stars born out of primordial hydrogen and helium will produce H II regions, which expand into a surrounding medium still of primordial constituents. So the temperature in these first H II regions around massive stars will be determined by bremsstrahlung, recombination radiation and bound-bound transitions either as follow up to recombination to excited levels of hydrogen and helium or induced by collisions (see the compilation of Katz et al. 1996, for instance). During the expansion of the ionized region down to pressure balance with the surrounding medium or the end of the ionizing radiation, an ionization front will propagate and consume a large fraction of the ionizing photons. Assuming local ionization and thermal equilibrium inside the H II region, we derive temperatures ranging from 10^5 K in a dense inner He III region to an intermediate regime of $6 - 8\,10^4$ K for hot stars and a drop to $2 - 3\,10^4$ K for the main part of extended H II regions produced by all ionizing stars. The temperature drops to roughly 10^4 K as the ionization balance allows for a significant fraction of neutral hydrogen in the outermost parts. The evolution of an H II region to this stage takes approximately 10^6 years and has to be compared with the lifetime of the ionizing source.

Acknowledgements. TB and WJD acknowledge partial support by the *Deutsche Forschungsgemeinschaft* (DFG) through SFBs 328 and 439; TB acknowledges support through DAAD grant D/98/27005 (Die Arbeit wurde mit Unterstützung eines Stipendiums im Rahmen des gemeinsamen Hochschulsonderprogramms III von Bund und Ländern über den DAAD 2 ermöglicht.).

Appendix A: how to average Gaunt factors for free-free emission

The free-free emissivity is the density of electrons and ions multiplied by the differential cross section integrated over the initial velocity distribution $vf(v)$. We use the mean energy of the electrons

$$\langle \mathcal{E} \rangle = \int_0^\infty \mathrm{d}v\, \frac{mv^2}{2} f(v) \tag{A.1}$$

to obtain the scale-free kinetic energy of the final electrons

$$y = \left(mv_\mathrm{i}^2/2 - h\nu\right) / \langle \mathcal{E} \rangle \,. \tag{A.2}$$

The averaged Gaunt factor can be expressed in terms of a modified distribution function $\tilde{f}(v) = f(v)/v^2$ and gives

$$G(\nu, \tilde{f}) = \frac{\langle \mathcal{E} \rangle}{m} \int_0^\infty \mathrm{d}y\, g(\eta_\mathrm{i}, \eta_\mathrm{f}) \tilde{f}(v(y)) \tag{A.3}$$

where the velocity is a function of y. In the case of a thermal distribution we obtain

$$G(\nu,T) = \left(\frac{2m}{\pi kT}\right)^{1/2} e^{-h\nu/(kT)} \int_0^\infty g(\eta_\mathrm{i},\eta_\mathrm{f})\, e^{-y}\, \mathrm{d}y. \quad \text{(A.4)}$$

The standard form for the thermally averaged Gaunt factor is $G(\nu,T)$ divided by the average obtained from the semi-classical expression of Kramers and Wentzel. This leads to

$$g_\mathrm{ff} = \int_0^\infty g(\eta_\mathrm{i},\eta_\mathrm{f}) e^{-y}\, \mathrm{d}y. \quad \text{(A.5)}$$

The Gaunt factor g_ff does not contain the exponential $\exp\left[-h\nu/kT\right]$ of Eq. A.4 which arises as the integral over initial electron velocities is limited to $v_\mathrm{i}^2 > 2h\nu/m$.

References

Abramowitz M., Stegun I.A., 1972, In: Abramowitz M., Stegun I.A. (eds.) Handbook of Mathematical Functions. Dover Publications, New York, NY, USA

Altenhoff W., Mezger P.G., Wendker H., Westerhout G., 1960, Veröff. Univ.-Sternwarte Bonn 59, 48

Brussaard P.J., van de Hulst H.C., 1962, Rev. Mod. Phys. 34, 507

Cooper J., 1966, Rep.Prog.Phys. 29, 2

Gaunt J.A., 1930, Phil. Trans. R. Soc. London, Ser. A 229, 163

Grant I.P., 1958, MNRAS 118, 241

Karzas W.J., Latter R., 1962, ApJS 6, 167

Katz N., Weinberg D.H., Hernquist L., 1996, ApJS 105, 19

Kramers H.A., 1923, Phil. Mag. 46, 836

Menzel D.H., Pekeris C.L., 1935, MNRAS 96, 77

Mezger P.G., Henderson A.P., 1967, ApJ 147, 471

Mezger P.G., Smith L.F., Churchwell E., 1974, A&A 32, 269

Oster L., 1961, ApJ 134, 1010

Oster L., 1963, ApJ 137, 332

Oster L., 1970, A&A 9, 318

Osterbrock D.E., 1989, Astrophysics of Gaseous Nebulae and Active Galactic Nuclei. University Science Books, Sausalito, CA, USA

Rubin R.H., 1968, ApJ 154, 391

Scheuer P.A.G., 1960, MNRAS 120, 231

Storey P.J., Hummer D.G., 1995, MNRAS 272, 41

Seaton M.J., 1959, MNRAS 119, 81

Willner S.P., Becklin E.E., Visanathan N., 1972, ApJ 175, 699

Wynn-Williams C.G., Becklin E.E., Neugebauer G., 1972, MNRAS 160, 1